

# Phase Behavior and Rheological Properties of Polyamine-Rich Complexes for Direct-Write Assembly

Mingjie Xu<sup>†,‡</sup> and Jennifer A. Lewis<sup>\*,†,‡,§</sup>

Frederick Seitz Materials Research Laboratory, Chemical and Biomolecular Engineering Department, and Materials Science and Engineering Department, University of Illinois at Urbana–Champaign, Urbana, Illinois 61801

Received July 24, 2007. In Final Form: September 6, 2007

Polyamine-rich complexes are developed for microscale patterning of planar and 3-D structures by direct ink writing. The complexes are formed by mixing poly(allylamine) hydrochloride and poly(acrylic acid) sodium salt in water in a nonstoichiometric ratio. Their phase behavior, rheological properties, and coagulation behavior in alcohol–water reservoirs are characterized. Direct comparisons are made between these complexes, which are based on mixtures of linear polyelectrolytes, and prior observations of complexes composed of linear and highly branched chains. [Gratson, G. M.; Xu, M.; Lewis, J. A. *Nature* **2004**, *428*, 386. Gratson, G. M.; Lewis, J. A. *Langmuir* **2005**, *21*, 457–464.] The optimal polyamine-rich ink and reservoir compositions are identified for direct-write assembly of wavy, gradient, and 3-D microperiodic architectures.

## Introduction

Planar and three-dimensional (3-D) polymer scaffolds with microscale features may find potential application as tissue-engineering scaffolds,<sup>3–5</sup> novel membranes,<sup>6–8</sup> microfluidic networks,<sup>9</sup> and photonic band gap materials.<sup>10,11</sup> While photo-,<sup>12</sup> soft-,<sup>13,14</sup> and electron-beam lithographic<sup>15</sup> techniques are well-suited for patterning planar surfaces, they do not readily lend themselves to 3-D architectures.<sup>16</sup> To address this deficiency, multibeam interference lithography,<sup>17,18</sup> two-photon polymerization,<sup>19</sup> conformable phase mask lithography,<sup>16</sup> and direct ink writing (DIW) techniques<sup>1,2</sup> have recently been introduced for

precisely assembling polymers into 3-D microperiodic structures. Of these, only the latter approach offers the flexibility of assembling polyelectrolyte species in both periodic and arbitrary shapes.<sup>1,2,20</sup>

We recently demonstrated DIW of 3-D scaffolds from concentrated polyelectrolyte complexes (PECs).<sup>1,2</sup> Specifically, we created polyanion-rich complexes, by mixing poly(acrylic acid) (PAA) and polyethylenimine (PEI) in water, that are capable of flowing through micron-sized deposition nozzles and then rapidly coagulating in an alcohol-rich reservoir to maintain their filamentary shape (see Figure 1). Homogeneous inks are obtained by combining species of different molecular weight at nonstoichiometric charge group ratios under solution conditions that promote polyelectrolyte exchange reactions.<sup>2,21</sup>

Here, we explore polyelectrolyte complexes composed of an aqueous mixture of poly(allylamine) hydrochloride (PAH) and poly(acrylic acid) (PAA) to simultaneously broaden our understanding of the rich behavior of PECs as well as determine the generality of our ink design for direct-write assembly. Both PAH and PAA possess a linear backbone along which their respective ionizable groups are uniformly distributed. These highly complementary polyions likely adopt a “ladder-like” architecture during complex formation, as shown in Figure 2a. By contrast, PEI is expected to form an ionically cross-linked network with PAA due to its lower molecular weight and highly branched nature (see Figure 2b). By comparing observations made on PAH–PAA complexes to those reported previously for the PAA–PEI system, we gain new insight into how this molecular level structuring affects their phase behavior, rheological properties, and coagulation behavior. Finally, by optimizing both the PAH–PAA complex and alcohol–water reservoir compositions, we create PAH-rich inks suitable for microscale patterning of polymeric structures with wavy, gradient, and 3-D periodic architectures.

\* Corresponding author. E-mail address: jalewis@uiuc.edu.

<sup>†</sup> Frederick Seitz Materials Research Laboratory.

<sup>‡</sup> Chemical and Biomolecular Engineering Department.

<sup>§</sup> Materials Science and Engineering Department.

(1) Gratson, G. M.; Xu, M.; Lewis, J. A. *Nature* **2004**, *428*, 386.

(2) Gratson, G. M.; Lewis, J. A. *Langmuir* **2005**, *21*, 457–464.

(3) Griffith, L. G.; Naughton, G. *Science* **2002**, *295*.

(4) Karageorgiou, V.; Kaplan, D. *Biomaterials* **2005**, *26*, 5474–5491.

(5) Endler, E. E.; Duca, K. A.; Nealey, P. F.; Whitesides, G. M.; Yin, J. *Biotechnol. Bioeng.* **2003**, *81*, 719–725.

(6) Zhao, D. Y.; Yang, P. D.; Chmelka, B. F.; Stucky, G. D. *Chem. Mater.* **1999**, *11*, 1174.

(7) Liu, X. Y.; Bruening, M. L. *Chem. Mater.* **2004**, *16*, 351–357.

(8) Sullivan, D. M.; Bruening, M. L. *J. Am. Chem. Soc.* **2001**, *123*, 11805–11806.

(9) Theriault, D.; White, S. R.; Lewis, J. A. *Nat. Mater.* **2003**, *2*, 265–271.

(10) Fleming, J. G.; Lin, S. Y.; El-Kady, I.; Biswas, R.; Ho, K. M. *Nature* **2002**, *417*, 52–55.

(11) Lin, S. Y.; Fleming, J. G.; Hetherington, D. L.; Smith, B. K.; Biswas, R.; Ho, K. M.; Sigalas, M. M.; Zubrzycki, W.; Kurtz, S. R.; Bur, J. *Nature* **1998**, *394*, 251–253.

(12) Mooney, J. F.; Hunt, A. J.; McIntosh, J. R.; Liberko, C. A.; Walba, D. M.; Rogers, C. T. *Proc. Natl. Acad. Sci. U.S.A.* **1996**, *93*, 12287–12291.

(13) Whitesides, G. M.; Ostuni, E.; Takayama, S.; Jiang, X. Y.; Ingber, D. E. *Annu. Rev. Biomed. Eng.* **2001**, *3*, 335–373.

(14) Xia, Y.; Whitesides, G. M. *Annu. Rev. Mater. Sci.* **1998**, *28*, 153–184.

(15) Craighead, H. G. *Science* **2000**, *290*, 1532–1535.

(16) Jeon, S.; Park, J. U.; Cirelli, R.; Yang, S.; Heitzman, C. E.; Braun, P. V.; Kenis, P. J. A.; Rogers, J. A. *Proc. Natl. Acad. Sci. U.S.A.* **2004**, *101*, 12428–12433.

(17) Campbell, M.; Sharp, D. N.; Harrison, M. T.; Denning, R. G.; Turberfield, A. J. *Nature* **2000**, *404*, 53–56.

(18) Yang, S.; Megens, M.; Aizenberg, J.; Wiltzius, P.; Chaikin, P. M.; Russell, W. B. *Chem. Mater.* **2002**, *14*, 2831–2833.

(19) Cumpston, B. H.; Ananthavel, S. P.; Barlow, S.; Dyer, D. L.; Ehrlich, J. E.; Erskine, L. L.; Heikal, A. A.; Kuebler, S. M.; Lee, I. Y. S.; Mccord-Maughon, D.; Qin, J.; Rockel, H.; Rumi, M.; Wu, X.-L.; Marder, S. R.; Perry, J. W. *Nature* **1999**, *398*, 6722.

(20) Xu, M.; Gratson, G. M.; Duoss, E. B.; Sheperd, R. F.; Lewis, J. A. *Soft Matter* **2005**, *2*, 205–209.

(21) Bakeev, K. N.; Izumrudov, V. A.; Kuchanov, S. I.; Zezin, A.; Er, B.; Kabanov, V. A. *Macromolecules* **1992**, *25*, 4249–4254.

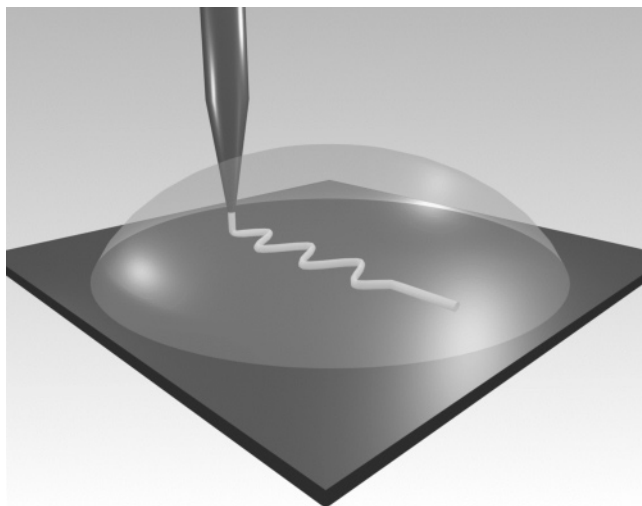


**Figure 1.** Schematic illustration of direct ink writing (not drawn to scale).

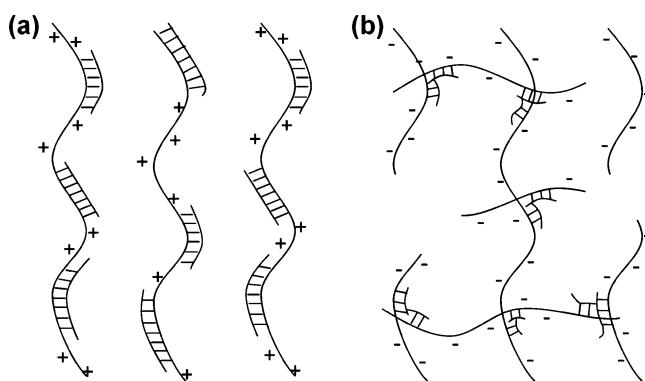


**Figure 2.** Schematic of the proposed (a) ladder-like structure for PAH-PAA complexes. PAH molecules are denoted by long chains and PAA by short parallel chains. (b) Scrambled salt structure for PAA-PEI complexes. PAA molecules are denoted by long crossing chains and PEI by short branched segments at the crossing points. The net charge groups of these nonstoichiometric complexes are denoted by + and - symbols, respectively.

## Experimental Section

**Materials System.** Poly(allylamine) hydrochloride (PAH) is a cationic polyelectrolyte composed of a linear backbone with one primary amine side chain per monomer unit. PAH ( $M_w \sim 60\,000$ ) (Polysciences, Inc., Warrington, PA) was supplied as a powder and used as-received for ink formulation. Poly(acrylic acid) sodium salt (PAA) is an anionic polyelectrolyte with a linear backbone comprised of one ionizable [COONa] group per monomer unit. PAA sodium salt ( $M_w \sim 1200$ ) (Aldrich Chemical, Milwaukee, WI) was supplied as a concentrated aqueous solution (45% by weight) and used as-received for ink formulation. Note, poly(acrylic acid) (PAA) sodium salt ( $M_w \sim 10\,000$ ) and polyethylenimine (PEI) ( $M_w \sim 600$ ) are used to formulate the PEI-PAA complexes described in ref 2, whose behavior serves as a benchmark for the current investigation. The coagulation reservoirs are prepared by mixing isopropyl alcohol (IPA) (ACS grade, Fisher Scientific, NJ), ethyl alcohol (Absolute, Aaper Alcohol and Chemical Co.), and deionized water at varying volumetric ratios.

**Phase Behavior.** Polyelectrolyte complexes are prepared by mixing appropriate amounts of PAH, PAA, and water to achieve the desired polymer concentration and charge group ratio ( $[\text{NH}_3^+]/[\text{COONa}]$ ). Immediately after mixing these constituents, an opaque precipitate forms. The mixtures are then equilibrated for several hours by magnetic stirring. Depending on their composition, they either yield a clear, soluble complex (single-phase) or phase separate

into a polymer-rich precipitate with a dilute polymer-poor supernatant (two-phase). Most single-phase complexes homogenize within 24 h of stirring. However, the homogenization time required increases dramatically as their composition approaches the two-phase region. If precipitates persist after 48 h, the complexes are defined as two-phase mixtures. Note, in these experiments, no attempt is made to control the solution pH, which varies from pH 2.5–3.3 in the PAH-rich region to pH 6–7.7 in the PAA-rich region.

**Ink Rheology.** The rheological properties of aqueous PAH-PAA complexes are determined using a controlled stress rheometer (Bohlin Instruments CVOR, East Brunswick, NJ). The viscosity measurements are acquired in controlled stress mode using a concentric cylinder geometry (C14, bob diameter of 14 mm and gap size of 0.7 mm). Data are collected as a function of shear stress ( $\tau$ ) in a logarithmically ascending series of discrete steps (0.05–50 Pa) with a 20 s delay after each data point.

The elastic shear modulus ( $G'$ ) of concentrated inks coagulated in deposition reservoirs of varying composition is measured in oscillatory mode using a cone and plate geometry (CP 4/40, cone diameter 40 mm with a  $4^\circ$  angle and gap size of  $150\ \mu\text{m}$ ). This geometry is adopted, because measurements cannot be carried out directly on deposited ink filaments. We estimate that a characteristic coagulation time of  $\sim 2$  h is necessary to allow a  $100\ \mu\text{m}$  polyelectrolyte film to undergo comparable solidification. These films are prepared by coating the plate with the polyelectrolyte complex of interest and then dipping the cone into this viscous fluid such that both surfaces are coated with  $\sim 90\ \mu\text{m}$  thick films. The coated cone and plate are then separated and placed in an alcohol/water coagulation reservoir (1 L) of varying composition for 2 h. Upon removal from the reservoir, the cone and plate fixtures are mounted on the rheometer and the coated surfaces are brought into contact and allowed to fuse together for 5 min. The test fixture is then sealed with the same coagulation solution, which serves as a solvent trap to minimize drying effects. The  $G'$  is acquired as a function of controlled stress at a frequency of 1 Hz with increasing amplitude sweep. All measurements are conducted at  $22\ ^\circ\text{C}$ .

Carbon-hydrogen-nitrogen (CHN) analysis is carried out on a representative polyelectrolyte ink ( $[\text{NH}_3^+]:[\text{COONa}] = 2:1$ ) before and after coagulation in deionized water and pure alcohol reservoirs. Coagulated samples are prepared by immersing the thick films in a given reservoir for 2 h, analogous to the procedure used for the rheological measurements. Solid powder samples are obtained by drying the films in an oven at  $100\ ^\circ\text{C}$  for 12 h to fully evaporate any remaining solvent. Their composition is measured using a CHN analyzer (CE440, Exeter Analytical, Inc., North Chelmsford, MA) and compared to known values for PAH and PAA to determine the final  $[\text{NH}_3^+]:[\text{COONa}]$  ratio after coagulation.

**Ink-Swelling Measurements.** The swelling behavior of PAH-rich complexes is studied by measuring their volume change upon exposure to reservoirs of varying composition. Approximately 500 mg of PAH-PAA ink (50 wt % polymer, 2:1 charge ratio) is placed in the bottom of each transparent scintillation bottle (1.5 cm in diameter and 5 cm in height). The reservoir solution (7 mL) is then gently added on top of the polyelectrolyte complex (3 mm in height) to initiate swelling. The sample height is monitored continuously during 72 h of immersion.

**Direct-Write Assembly.** Planar and 3-D polymer scaffolds with microscale features are assembled by DIW using a robotic deposition apparatus (ABL9000, Aerotech Inc., Pittsburgh, PA). The ink is housed in a syringe (barrel diameter = 4.6 mm; EFD Inc., East Providence, RI) and deposited through a pulled borosilicate glass nozzle ( $\mu$ -Tip, World Precision Instruments, Inc., Sarasota, FL). Pressure (20–50 psi) (800 Ultra dispensing system, EFD Inc.) is applied to maintain a constant volumetric flow rate that matches the desired deposition speed (40–500  $\mu\text{m/s}$ ). The ink delivery system is mounted onto the moving  $x$ - $y$ - $z$  micropositioner for agile printing onto a stationary substrate. The PAH-PAA ink (50% by weight, 2:1 charge ratio) is deposited into a coagulation reservoir ( $\sim 300\ \mu\text{L}$ ) consisting of 80% isopropyl alcohol, 9% ethanol, and 11% water. As the ink exits the nozzle, it rapidly coagulates ( $\sim 1$  ms) to form a continuous, rod-like filament that retains its shape.

Wavy microperiodic structures are patterned by depositing an array of sinusoidal-like filaments ( $1\ \mu\text{m}$  in diameter) within the  $x$ - $y$  plane, as illustrated in Figure 1. Every filament consists of 14 tangential arcs with alternating centers. Each arc has a horizontal span of  $21.7\ \mu\text{m}$  and a radius of  $30.6\ \mu\text{m}$ . The road width between the filament centers is  $8\ \mu\text{m}$ , which is twice the height of each arc ( $\sim 4\ \mu\text{m}$ ). The total build time is  $\sim 1.5$  min at a writing speed of  $150\ \mu\text{m/s}$  for a  $300\ \mu\text{m} \times 300\ \mu\text{m}$  structure. 3-D gradient structures are assembled by patterning a parallel array of rod-like filaments, whose separation distance increases from 5 to  $20\ \mu\text{m}$  in increments of  $0.375\ \mu\text{m}$  between adjacent lines. Upon completion of a given layer, the deposition nozzle is raised  $1\ \mu\text{m}$  in the  $z$ -direction and another layer of parallel rods is patterned in the orthogonal direction to form self-supporting features. This process is repeated until the entire 3-D structure is patterned. The approximate build time is 7 min for a three-layer,  $200\ \mu\text{m} \times 200\ \mu\text{m}$  structure at a printing speed of  $150\ \mu\text{m/s}$ . Three-dimensional microperiodic structures with a tetragonal geometry are assembled in a similar manner with a fixed separation distance between filaments (or road width) of  $7\ \mu\text{m}$ . Finally, 3-D triangular lattices are patterned by depositing an array of parallel filaments with a road width of  $6\ \mu\text{m}$ . Within each plane, the filament length is confined by an equilateral triangle with an edge length of  $160\ \mu\text{m}$ . Subsequent layers are patterned in a similar fashion except that the filament orientation is rotated by  $120^\circ$ . The approximate build time for each 9-layer structure is 2.5 min at a printing speed of  $150\ \mu\text{m/s}$ .

The coagulation reservoir is maintained at a constant composition by continuously circulating fresh solution via a symmetric syringe pump (Harvard Twin syringe pump 33, Harvard Apparatus, Holliston, MA). Scaffolds patterned within this reservoir are able to maintain their structural integrity during the printing and drying process. Polyamine-rich structures with microscale features are dried in a low-humidity environment (15–28%), followed by heating from 25 to  $80\ ^\circ\text{C}$  at  $5\ ^\circ\text{C}/\text{min}$  (2 h hold) and then heating to  $180\ ^\circ\text{C}$  at  $5\ ^\circ\text{C}/\text{min}$  (2 h hold) to promote amide bond formation between the  $[\text{NH}_x]$  and  $[\text{COONa}]$  groups.<sup>20,22</sup> These partially cross-linked scaffolds have improved structural integrity, which facilitates their subsequent handling.<sup>20</sup>

**Oxygen Plasma Treatment.** The morphology of partially cross-linked ink filaments is investigated using oxygen plasma ablation (Reactive Ion Etching, Plasma-Therm 720 series, Wernersville, PA). Under relatively isotropic conditions (200 mTorr, 20 sccm, 100 W), ink filaments are gradually etched to reveal their underlying structure. The partially etched filaments are then imaged using Hitachi SEM 4700, and their heights are determined by surface profilometry (Sloan Dektak<sup>3</sup> ST, Santa Barbara, CA).

## Results and Discussion

**Phase Behavior of PAH–PAA Complexes.** The PAH–PAA– $\text{H}_2\text{O}$  phase diagram is shown in Figure 3a. Pure PAH and PAA solutions reside along the binary polyelectrolyte–water tie lines. These solutions are homogeneous fluids over the entire compositional range explored. Upon mixing PAH and PAA in deionized water, dramatic differences in their phase behavior are observed. The PAH–PAA complexes undergo phase separation regardless of the polycation-to-polyanion ratio when the polyamine concentration is less than  $c^* \sim 0.16\ \text{g/mL}$ , where  $c^*$  denotes the dilute-to-semidilute transition for the pure PAH solutions. Such complexes phase separate into a polymer-rich precipitate and a polymer-poor supernatant fluid even under the most dilute conditions. By contrast, their PAA–PEI counterparts formed suspensions of colloidal particles<sup>2</sup> under analogous conditions, when the PEI concentration was less than or equivalent to the PAA concentration in solution. At intermediate polymer concentrations ( $\sim 20$ – $40\ \text{wt}\%$ ), the two-phase region observed in the PAH–PAA– $\text{H}_2\text{O}$  phase diagram is nearly symmetrical across

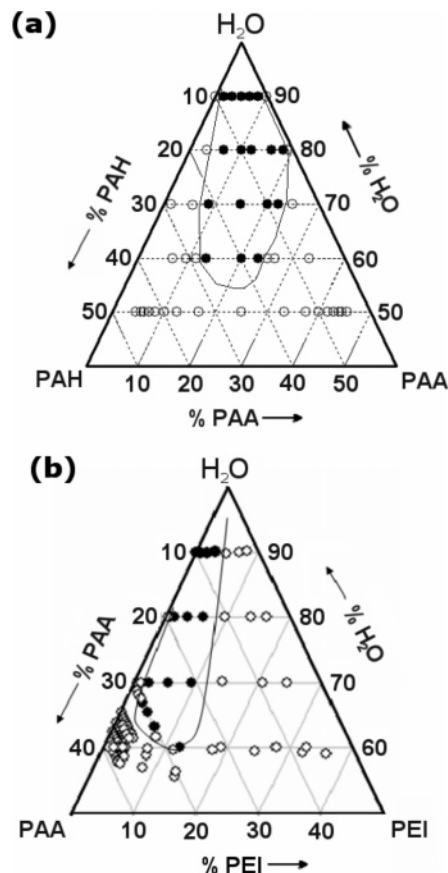


**Figure 3.** (a) PAH–PAA– $\text{H}_2\text{O}$  phase diagram showing both the single-phase region composed of homogeneous soluble complexes (○) and the two-phase region composed of a polymer-rich precipitate and a polymer-poor supernatant (●). (Note: The solution pH ranges from 2.5–3.3 in the PAH-rich region to pH 6–7.7 in the PAA-rich region.) (b) PAA–PEI– $\text{H}_2\text{O}$  phase diagram showing (○) single-phase regions of macroscopically homogeneous, soluble complexes and (●) two-phase regions comprised of a turbid suspension of stable complex colloidal particles in a polymer-poor fluid (below  $c^*$ ) or a precipitated complex with a polymer-poor supernatant fluid (above  $c^*$ ) (Note: the solution pH ranged from pH 3.5–4 in the PAA-rich region to pH  $\sim 11$  in the PEI-rich region.) (from ref 2).

the charge equivalence line. Similar behavior is also observed for the PAA–PEI– $\text{H}_2\text{O}$  system; however, due to the higher number of charge groups per unit mass of PEI, this two-phase region is shifted toward PAA-rich compositions<sup>2</sup> (Figure 3b). In both cases, the observed PEC phase behavior is in good agreement with recent predictions by computer simulations.<sup>23</sup>

At higher polyelectrolyte concentrations ( $> 45\ \text{wt}\%$ ), a single-phase region emerges within the PAH–PAA– $\text{H}_2\text{O}$  phase diagram (see Figure 3a). Homogeneous soluble complexes form due to enhanced polyelectrolyte exchange reactions that promote the structural rearrangement of initially aggregated species in solution.<sup>21,24</sup> Polyelectrolyte exchange reactions are known to be highly dependent on polymer concentration, mixing ratio, ionic strength, and pH.<sup>25</sup> For the experimental conditions explored, homogeneous PEC inks suitable for direct-write assembly are produced from concentrated PAH-rich complexes (50 wt % of polymer) possessing a charge group  $[\text{NH}_x]:[\text{COONa}]$  ratio of 2:1.

(23) Skepo, M.; Linse, P. *Macromolecules* **2003**, *36*, 508–519.

(24) Izumrudov, V. A.; Savitskii, A. P.; Zezin, A. B.; Kabanov, V. A. *Polym. Sci. U.S.S.R.* **1984**, *26*, 1930–1939.

(25) Zintchenko, A.; Rother, G.; Dautzenberg, H. *Langmuir* **2003**, *19*, 2507–2513.

(22) Harris, J. J.; Derosé, P. M.; Bruening, M. L. *J. Am. Chem. Soc.* **1999**, *121*, 1978–1979.

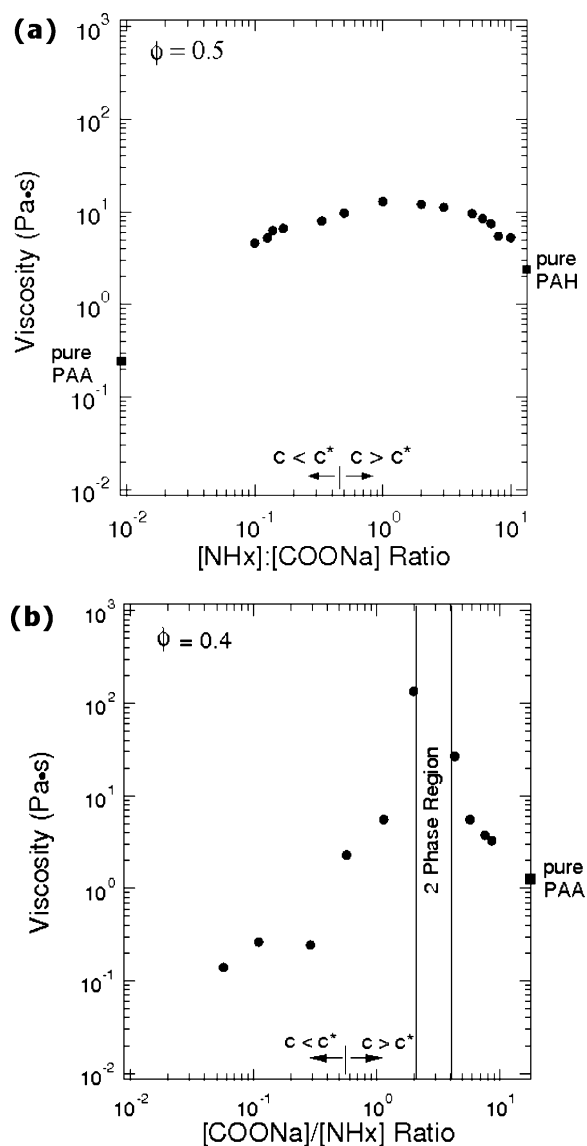


**Figure 4.** (a) Log–log plot of the initial viscosity of concentrated PAH–PAA inks (50 wt %) as a function of varying  $[\text{NH}_x]:[\text{COONa}]$  ratio. (b) log–log plot of the initial ink viscosity for concentrated PAA–PEI complexes (40 wt %) with varying  $[\text{COONa}]/[\text{NH}_x]$  ratio (from ref 2). Note, the respective dilute-to-semidilute concentrations ( $c^*$ ) of pure PAH and PAA solutions are denoted on the x-axis of each plot.

**Initial Ink Rheology.** The viscosity of concentrated PAH–PAA complexes (50 wt % in solution) as a function of varying  $[\text{NH}_x]:[\text{COONa}]$  ratio is shown in Figure 4a. Under these conditions, PAH–PAA complexes form homogeneous solutions that exhibit slight shear-thinning behavior. These complexes experience a rather modest rise in ink viscosity at shear rate  $\sim 1 \text{ s}^{-1}$  when their composition changes from pure PAH ( $\sim 5 \text{ Pa s}$ ) to 1:1 PAH–PAA complex ( $\sim 13 \text{ Pa s}$ ), as shown in Figure 4a. By contrast, the PAA–PEI complexes studied previously exhibited Newtonian behavior<sup>2</sup> and experienced a two order of magnitude rise in viscosity, from 1 to 100 Pa s, as their composition approaches the two-phase boundary<sup>2,26</sup> (Figure 4b). To better understand these differences, we carried out viscosity measurements on PAH–PAA complexes of a lower total polyelectrolyte concentration (42.5 wt % in solution), whose composition is varied across the two-phase boundary line.

Interestingly, no dramatic rise in viscosity is observed under these conditions (data not shown). Indeed, we find that their viscosity slowly increases as the PEC composition approaches the charge equivalence line, in a manner analogous to that of the PAH–PAA complexes of higher polyelectrolyte concentration (50 wt % in solution).

In concentrated mixtures of oppositely charged polyelectrolytes, electrostatic interactions are the main driving force for molecular-level structuring and, hence, the sharp rise in viscosity observed for the PAA–PEI inks.<sup>26</sup> Depending on its size, charge density, and architecture, a given polyion can either associate with several oppositely charged species serving as a cross-linker that reinforces chain entanglement or it can complex with single (or a few) species, yielding a loose network of lower viscosity (see Figure 2). Due to its low molecular weight and highly branched nature, PEI is more likely to form an ionically cross-linked network with PAA than PAH, which has a linear architecture. The viscosity data suggests that PAH–PAA complexes exhibit less molecular-level structuring than their PAA–PEI counterparts, in good agreement with the proposed association between these polyions.

By regulating the  $[\text{NH}_x]:[\text{COONa}]$  ratio of the PAH–PAA complexes, their viscosity can be tailored to facilitate flow through micron-sized deposition nozzles. Gratson<sup>2</sup> showed that the pressure required to maintain a desired volumetric flow rate through a tapered microcapillary nozzle is directly proportional to the ink viscosity and inversely proportional to the nozzle diameter. Using an approximation of the Hagen–Poiseuille model,<sup>2</sup> we estimate that the optimal ink viscosity ranges from 7.2 to 18.1 Pa s for the DIW conditions employed in this study (i.e., 1  $\mu\text{m}$  deposition nozzle, 150  $\mu\text{m/s}$  deposition speed, and an applied pressure of 20–50 psi). For the compositional range explored, we find that PAH-rich complexes with a charge group ratio of 2:1 to 7:1  $[\text{NH}_x]:[\text{COONa}]$  satisfy these requirements. We therefore utilize a PAH–PAA complex (50 wt % in solution) with a  $[\text{NH}_x]:[\text{COONa}]$  ratio of 2:1 and a viscosity of 12 Pa s to demonstrate the microscale patterning of polyamine-rich structures via DIW.

**Coagulation and Swelling Behavior.** PAH–PAA complexes undergo coagulation when deposited into a reservoir composed of three miscible liquids, isopropyl alcohol (IPA), ethanol, and deionized water. The observed rise in elasticity depends strongly on the reservoir composition, as shown Figure 5a, for a PAH–PAA complex (50 wt % in solution) with a  $[\text{NH}_x]:[\text{COONa}]$  ratio of 2:1. Prior to coagulation, this complex (or ink) exhibits a shear elastic modulus ( $G'$ ) of  $\sim 10 \text{ Pa}$ . Upon immersion in pure water, its elasticity remains roughly the same as observed in its initial state. When coagulated in a reservoir of increasing alcohol content, the elastic modulus slowly rises to a value of 800 Pa at 40 vol % alcohol and remains at this value for reservoir compositions between 40 and 80 vol % alcohol. At even higher alcohol concentrations ( $> 80 \text{ vol } \%$ ), the elasticity increases rapidly to a maximum value of  $4 \times 10^5 \text{ Pa}$  in pure alcohol. A reservoir composed of 89 vol % alcohol is deemed optimal, because it yields coagulated PAH-rich ink filaments that are elastic enough to span unsupported regions of a structure, yet still flexible enough to flow through a micron-sized deposition nozzle.

Upon initial exposure to pure water, the PAH–PAA complex turns white, indicating that coagulation is occurring. Over time, however, the coagulated ink swells to more than three times its initial volume (Figure 6a) without a significant change in elasticity. Dramatic swelling has been reported previously for multilayer films composed of weak polyelectrolytes. For example, Mendelsohn et al. reported that PAH–PAA multilayers assembled

(26) Liu, R. C. W.; Morishima, Y.; Winnik, F. M. *Macromolecules* **2001**, *34*, 9117–9124.

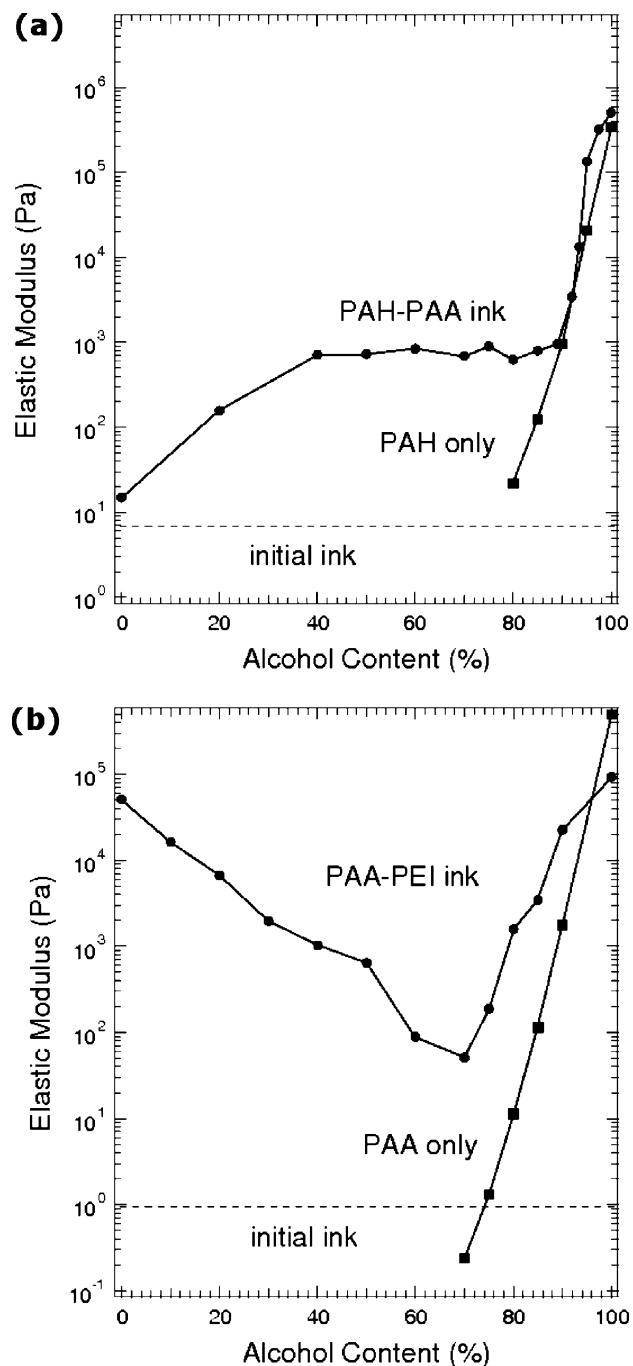


**Figure 5.** (a) Semilog plot of the elastic modulus of the coagulated PAH–PAA inks (●) (50 wt % with a  $[\text{NH}_4^+]:[\text{COONa}]$  ratio of 2:1) as a function of the alcohol content in the deposition reservoir. For comparison, the elastic modulus of a PAH solution (50 wt %) coagulated in the same reservoirs is also shown (■). (b) Semilog plot of the elastic modulus of concentrated PAA–PEI inks (●) (40 wt % with a 5.7:1  $[\text{COONa}]/[\text{NH}_4^+]$  ratio) as a function of alcohol content in the deposition reservoir. For comparison, the elastic modulus of a PAA solution (40 wt %) coagulated in the same reservoirs is also shown (■) (from ref 2). The ink elastic modulus before coagulation is denoted by the horizontal dotted line in both plots.

by electrostatic layer-by-layer assembly swelled to more than twice their initial thickness when exposed to a pH 2.5 solution.<sup>27</sup> Most recently, Itano et al. reported that PAH-sulfonated polystyrene (SPS) multilayer films assembled at high pH<sup>28</sup>

(27) Mendelsohn, J. D.; Barrett, C. J.; Chan, V. V.; Pal, A. J.; Mayes, A. M.; Rubner, M. F. *Langmuir* **2000**, *16*, 5017–5023.

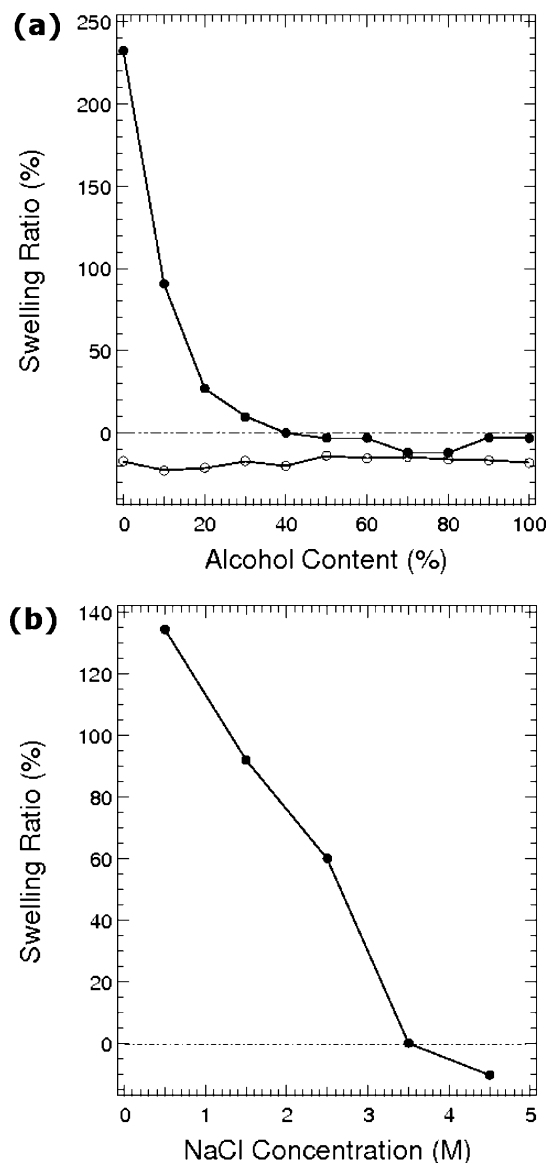


**Figure 6.** (a) Swelling behavior of PAH–PAA ink (●) (50 wt % with a 2:1  $[\text{NH}_4^+]:[\text{COONa}]$  ratio) and PAA–PEI (○) (40 wt % with 1:5.7  $[\text{NH}_4^+]:[\text{COONa}]$  ratio) as a function of alcohol content. (b) Swelling behavior of PAH–PAA ink (●) (50 wt % with a 2:1  $[\text{NH}_4^+]:[\text{COONa}]$  ratio) as a function of salt concentration in the reservoir. In both plots, the swelling ratio,  $R = (V_{\text{final}} - V_{\text{initial}})/V_{\text{initial}} \times 100\%$ .

exhibited a 4-fold increase in thickness when swelled in deionized water. By contrast, dramatic swelling is not observed for the PAA–PEI system (also shown in Figure 6a).

The coagulation and swelling behavior of the PAH–PAA complex is influenced by the degree of protonation of amine groups along the PAH chains<sup>30</sup> as well as their ladder-like architecture.<sup>29</sup> Upon immersion in pure water, significant swelling occurs as counterions diffuse from the PAH–PAA complex into the surrounding reservoir,<sup>2</sup> thereby inducing an enhanced electrostatic repulsion between ladder-like chains. This mechanism is further supported by our observation that swelling of this PAH–PAA complex is dramatically suppressed upon adding salt to the reservoir (Figure 6b). In sharp contrast, the PEI–PAA complex is believed to adopt a “scrambled salt” architecture.<sup>27,29</sup> Hence, as counterions diffuse into the water reservoir, the PAA–

(28) Itano, K.; Choi, J. Y.; Rubner, M. F. *Macromolecules* **2005**, *38*, 3450–3460.

(29) Philipp, B.; Dautzenberg, H.; Linow, K. J.; Kotz, J.; Dawydoff, W. *Prog. Polym. Sci.* **1989**, *14*, 91–172.

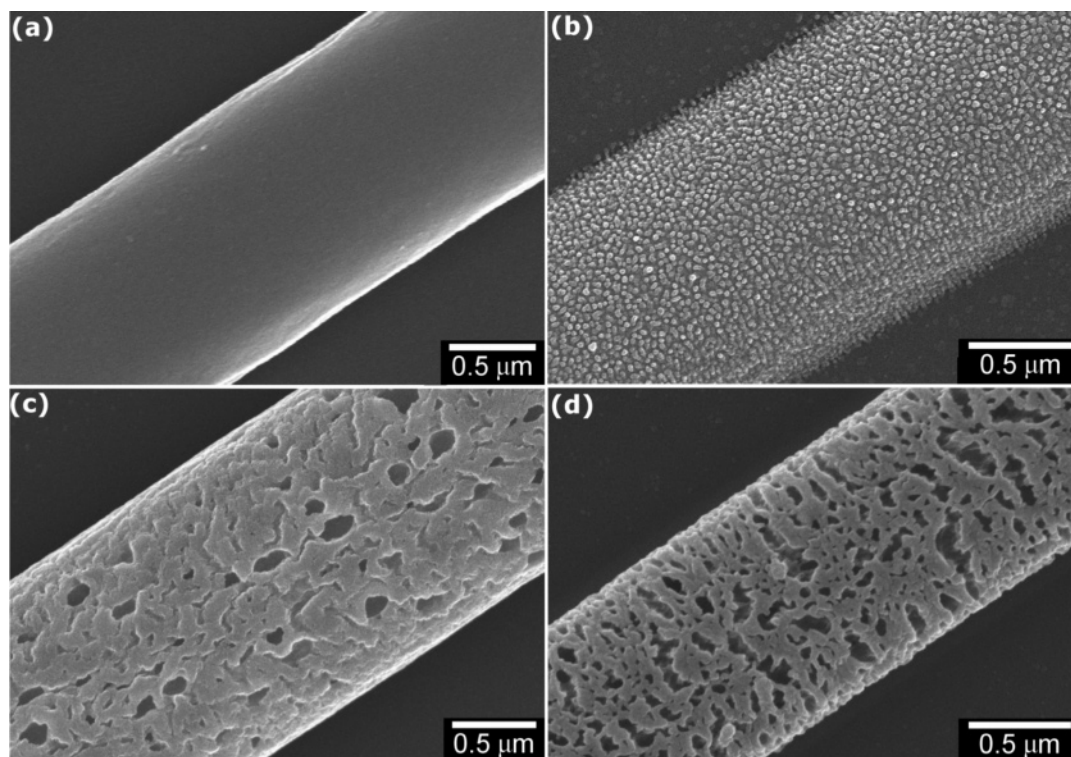


**Figure 7.** SEM images of PAH-PAA ink filaments as a function of oxygen plasma etching time: (a) 0, (b) 25, (c) 55, (d) 85 s.

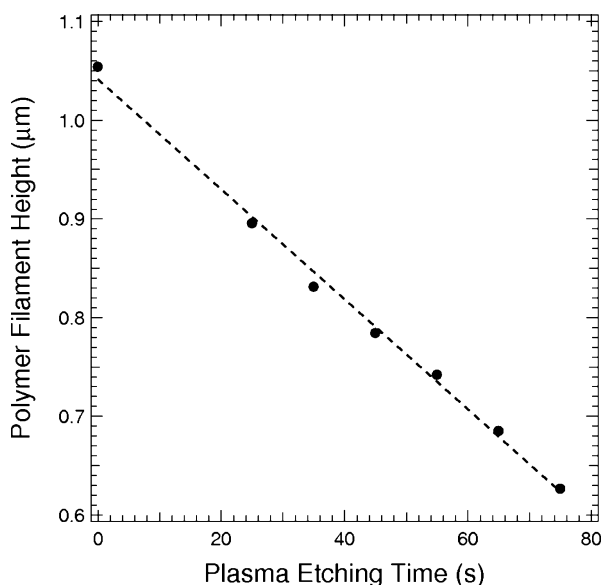


**Figure 8.** PAH-PAA ink filament height as a function of oxygen plasma etching time.

PEI complex retains its highly cross-linked network<sup>29,30</sup> due to enhanced electrostatic attractions between oppositely charged “linkers”. This is reflected by a dramatic rise in elasticity ( $\sim 4$  orders of magnitude) of the PAA-PEI complex, which is not observed for the PAH-rich complex under analogous conditions (see Figure 5).

Chemical (CHN) analysis shows that the PAH-PAA complex maintains its initial charge group ratio upon immersion in pure water. This behavior differs from that reported previously for the PAA-PEI complex, in which both excess PAA chains and counterions diffuse into the surrounding reservoir.<sup>2</sup> In fact, although their initial charge group ratio differs considerably, 2:1

vs 5.7:1, both PAH-PAA and PAA-PEI complexes adopt a similar final charge group ratio of 2.5:1 and 2:1, respectively, upon coagulation in pure water.

As the alcohol content within the reservoir increases, the coagulation behavior of PAH-PAA and PAA-PEI complexes initially exhibit opposite trends (see Figure 5). The PAH-PAA complex displays a steady rise in ink elasticity as the alcohol content increases from 0 to 40 vol %, in good agreement with the concurrent decrease in its extent of swelling. Simultaneously, counterion condensation<sup>31</sup> is promoted, which screens the electrostatic attractions<sup>2,32</sup> between oppositely charged polyelectrolytes. By contrast, this effect reduces the elasticity of the PAA-PEI complex, since it does not undergo swelling in any reservoir. At higher alcohol concentrations (40–80 vol %), PAH-PAA complex no longer experiences swelling and counterion condensation is further promoted, leading to a plateau in the ink elasticity. Finally, at even higher alcohol contents ( $> 80$  vol %), ink coagulation is driven solely by solvent quality effects<sup>2,32</sup> in both PAH-PAA and PAA-PEI complexes, yielding a sharp rise in their elasticity. In fact, even pure PAH and PAA solutions undergo a similar rise in elasticity in alcohol-rich reservoirs (see Figure 5). In each case, strong coagulation is dominated by hydrophobic interactions between polyion chains.<sup>33</sup>

**Ink Filament Morphology.** The underlying morphology of PAH-rich filaments coagulated in an alcohol-rich reservoir (89 vol % alcohol) is revealed by oxygen plasma etching.<sup>34–36</sup> Prior to etching, the as-patterned, partially cross-linked filaments have a smooth surface morphology, as shown in Figure 7a. After a short etching time (25 s), small islands that are approximately

(31) Manning, S. G. *Acc. Chem. Res.* **1979**, *12*, 443–449.

(32) Poptoshev, E.; Schoeler, B.; Caruso, F. *Langmuir* **2004**, *20*, 829–834.

(33) Dobrynin, A. V.; Rubinstein, M. *Macromolecules* **2001**, *34*, 1964–1972.

(34) Weigel, T.; Schulz, E.; Makschin, W.; Albrecht, W.; Klue, P.; Grobe, V. *Acta Polym.* **1988**, *39*.

(35) Fritzsche, A. K.; Armbruster, B. L.; Fraundorf, P. B.; Pellegrin, C. J. *J. Appl. Polym. Sci.* **1990**, *39*, 1915–1932.

(36) Fritzsche, A. K.; Cruse, C. A.; Kesting, R. E.; Murphy, M. K. *J. Appl. Polym. Sci.* **1990**, *40*, 19–40.

(30) Kim, D.; Park, K. *Polymer* **2004**, *45*, 189–196.

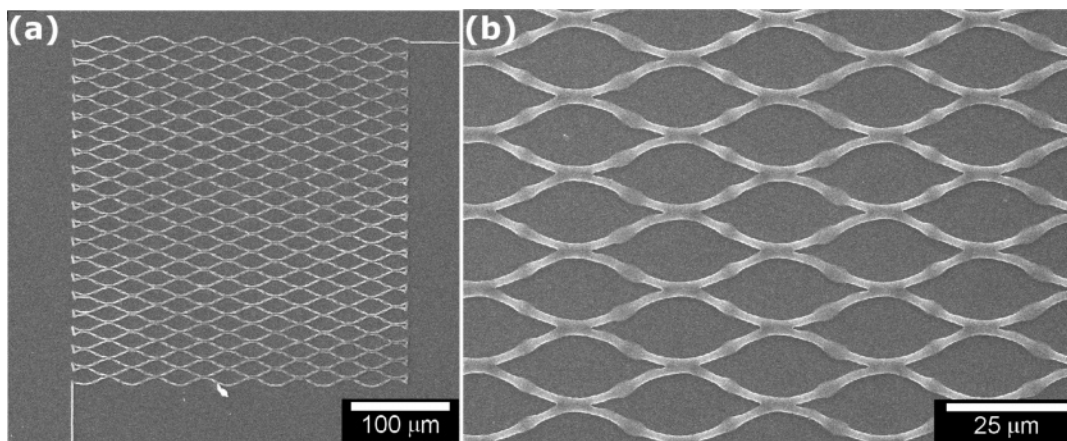


**Figure 9.** SEM images of a wavy pattern assembled by DIW. (a) Low magnification view showing overall structure and (b) higher magnification view of sinusoidal-like, polyamine-rich filaments.

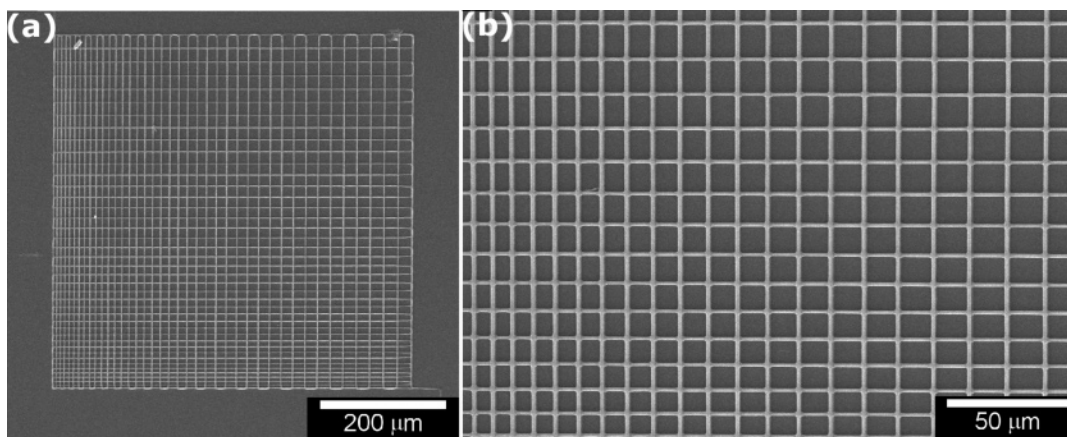


**Figure 10.** SEM images of a gradient structure with a road width that varies from 5 to 20  $\mu\text{m}$ . (a) Low magnification view showing overall structure and (b) higher magnification view of parallel, polyamine-rich filaments.

70–100 nm in size are observed on the filament surface (Figure 7b), which may arise due to preferential etching<sup>37</sup> of regions of low amide cross-link density. Upon completely removing the surface layer, their underlying porous morphology is revealed (Figure 7c). After further plasma etching, the voids grow in size (Figure 7d) and undergo some surface roughening.<sup>37,38</sup> We determine the etching rate by measuring the ink filament height as a function of time and find it to be roughly 5 nm/s (Figure 8) for these experimental conditions.

The dense outer surface and internal voids observed for PAH-rich filaments coagulated in alcohol-rich reservoirs are analogous to features found in asymmetric membranes,<sup>39,40</sup> which undergo phase inversion during their formation. Under poor solvent conditions, a homogeneous polymer solution phase separates into a polymer-rich matrix and a polymer-poor fluid,<sup>39,41</sup> the latter of which gives rise to internal voids upon drying. A dense outer layer (or skin) forms because rapid gelation at the filament–reservoir interface<sup>39–41</sup> inhibits phase separation. Hence, we can tune both the filament roughness and specific surface area by controlling their coagulation as well as postetching conditions. We anticipate that 3-D structures composed of highly porous,

polyelectrolyte filaments may be quite desirable for applications such as membranes<sup>39,40</sup> and tissue engineering scaffolds.<sup>3–5</sup>

**Direct-Write Assembly of Wavy, Gradient, and 3-D Microperiodic Structures.** A concentrated PAH-rich complex ( $\sim 50$  wt % with a  $[\text{NH}_x]:[\text{COONa}]$  ratio of 2:1) is utilized as an ink for direct-write assembly of planar and 3-D microperiodic structures. Under the optimized conditions identified by this work, the ink is flexible enough to flow through fine-sized deposition nozzle, yet undergoes rapid coagulation to yield self-supporting filaments.

Planar structures composed of wavy filaments are assembled by depositing an array of sinusoidal-like filaments. By controlling the height and horizontal span of each patterned feature as well as the road width between parallel filaments, a variety of wavy periodic structures can be created. As one example, we created the fish-net pattern shown in Figure 9, in which each sinusoidal-like filament is shifted by  $\pi$  such that it is in contact with the minimum and maximum amplitudes of its respective neighbors.

Gradient structures are also patterned by DIW of the PAH-rich ink, which may be well-suited for directing cell-scaffold interactions.<sup>5</sup> By way of demonstration, we created a 3-D gradient structure whose separation distance between adjacent filaments varies from 5 to 20  $\mu\text{m}$ , as shown in Figure 10. Within each layer, the filament separation distance is increased in increments of 0.375  $\mu\text{m}$  between adjacent rods. By taking advantage of the great flexibility of DIW and the well-defined chemistry of the

(37) Cvelbar, U.; Mozetic, M.; Klanjssek-Gunde, M. *IEEE Trans. Plas. Sci.* **2005**, *33*, 236–237.

(38) Teshima, K.; Sugimura, H.; Takano, A.; Inoue, Y.; Takai, O. *Chem. Vap. Deposition* **2005**, *11*, 347–349.

(39) Koros, W. J.; Fleming, G. K. *J. Membr. Sci.* **1993**, *83*, 1–80.

(40) Broens, L.; Altena, F. W.; Smolders, C. A. *Desalination* **1980**, *32*, 33–45.

(41) Altinkaya, S. A.; Yenal, H. *BioChem. Eng. J.* **2006**, *28*, 131–139.

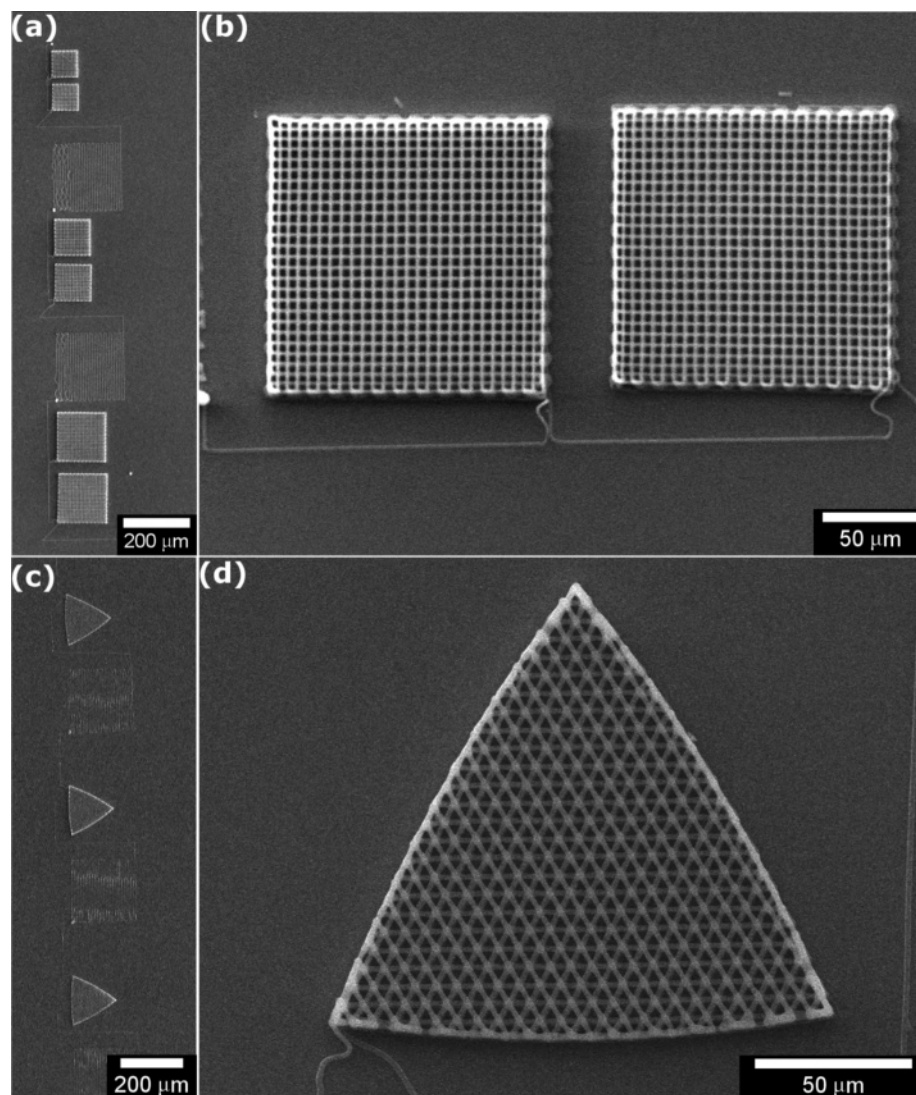


**Figure 11.** SEM images of 3-D microperiodic structures assembled via DIW. (a) A series of structures with simple tetragonal symmetry. From top to bottom, the edge length increases from 80 to 120 to 160  $\mu\text{m}$ , respectively. (b) Higher magnification view of tetragonal structures with six (right) and eight (left) layers. (c) A series of nine-layer triangular-shaped structures whose edge length equals 160  $\mu\text{m}$ . (d) Higher magnification view of triangular structure composed of polyamine-rich filaments.

polyelectrolyte filaments, our approach offers the potential to create a variety of scaffold architectures suitable for tissue engineering.

As a final example, we created 3-D microperiodic scaffolds with either a simple tetragonal or triangular geometry. Each 3-D tetragonal lattice consists of parallel arrays of rods that are oriented orthogonally between layers (Figure 11a,b). Each 3-D triangular lattice (Figure 11c,d) is comprised of nine layers of parallel rods that are confined within a triangular shape. The rods are orientated at  $120^\circ$  with respect to the previous layers. As a result, this structure is repeated every three layers in the  $z$  direction. To enable continuous printing of several structures, multiple lead-in and exit lines are utilized between structures to allow fine-tuning of the nozzle position and to ensure proper spacing between structures. In related work, we have recently demonstrated that such scaffolds may serve as templates for biomimetic mineralization of silica–organic hybrid structures<sup>20</sup> as well as photonic crystals with an inverse woodpile architecture.<sup>42,43</sup>

(42) Gratson, G. M.; García-Santamaría, F.; Lousse, V.; Xu, M.; Fan, S.; Lewis, J. A.; Braun, P. V. *Adv. Mater.* **2006**, *18*, 461–465.

(43) García-Santamaría, F.; Xu, M.; Lousse, V.; Fan, S.; Lewis, J. A.; Braun, P. V. *Adv. Mater.* **2007**, *19*, 1567–1570.

## Conclusions

We have developed concentrated polyamine-rich complexes suitable for direct ink writing of wavy, gradient, and 3-D microperiodic structures. By carefully tuning the ink and reservoir composition, homogeneous inks have been produced with the desired flow and coagulation behavior to enable microscale patterning. Our observations not only demonstrate the generality of this ink design but provide additional insights regarding the rich phase behavior, rheological properties, and coagulation behavior of polyelectrolyte complexes. The ability to construct planar and 3-D structures of arbitrary design opens up a facile avenue for fabricating novel membranes, tissue engineering scaffolds, photonic crystals, and sensors.

**Acknowledgment.** This material is based on work supported by the U.S. Army Research Office MURI program (Award no. DAAD19-03-1-0227) and the Air Force Office of Scientific Research under Award No. FA9550-05-1-0092 Subaward No. E-18-C45-G1). This work benefited greatly from access to the FSMRL Center for Microanalysis of Materials (CMM), which is partially supported by the U.S. Department of Energy under grants DE-FG02-07ER46453 and DE-FG02-07ER46471.